

Received March 17, 2022, accepted April 2, 2022, date of publication April 12, 2022, date of current version May 6, 2022.

Digital Object Identifier 10.1109/ACCESS.2022.3166889

Robust Design Scheme of C-Type Filter Considering Harmonic Dynamic Characteristics of Traction Power Supply System

HEXIANG WU¹, LIYONG ZENG¹, QINGSHUO REN^{1,2}, AND LEI AI²

¹China Railway Signal & Communication (Changsha) Railway Traffic Control Technology Company Ltd., Changsha 410006, China

²School of Electrical Engineering, Southwest Jiaotong University, Chengdu 610031, China

Corresponding author: Qingshuo Ren (renqingshuo@my.swjtu.edu.cn)


This work was supported in part by the Applied Basic Research Project of Sichuan province under Grant 2021YJ0062 and in part by the Postdoctoral Science Foundation of China under Grant 2020M683350.

ABSTRACT The passive filters are widely used in the harmonic control of traction power supply system. However, high-speed trains have many types and frequent working conditions, which result in random dynamic characteristics of the harmonic spectrum of the trains. Moreover, the rapid change in harmonic injection position leads to changes in the harmonic transmission characteristics of the system. So it is difficult for passive filters to fully compensate the harmonics. Meanwhile, the existing method adopts an approximate tuning-frequency calculation formula, which makes it difficult to accurately control its filtering performance. First of all, by deriving an accurate tuning-frequency expression, this study reveals the influence of component parameters on the tuning-frequency and the possibility of tuning-frequency disappearance. Subsequently, based on the impedance-frequency index, which can describe the overall distribution of harmonics, the improved firefly algorithm is used to obtain a robust optimization design of the parameters of the C-type filter. The calculation example analysis shows that the proposed scheme has strong adaptability to harmonic random dynamic characteristics and a better filtering effect than the existing design methods, which is more suitable for a traction power supply system with strong harmonic random dynamic characteristics.

INDEX TERMS Traction power supply system, harmonics, c-type filter, robust design.

I. INTRODUCTION

With the rapid development of large-scale high-speed railways in China, the harmonics and resonance of high-speed railway traction power supply systems (TPSS) are increasingly serious. On the one hand, Harmonic will cause the increasing system loss, insulation aging of equipment and interference the communication lines [1]. On the flip side, there will be severe harmonic resonance in the specific frequency, which will lead to resonance overvoltage, affecting the normal operation of equipment and even burning the equipment. For example, When the Guzhen Substation supplied power to Bengbu depot on the Beijing-Shanghai High Speed Railway in 2011, resonant overvoltages occurred many times, which resulted multiple main circuit breaker trips and caused lightning arrester damage [2]. Therefore, the suppression of TPSS harmonic and resonance is extremely important.

The associate editor coordinating the review of this manuscript and approving it for publication was Dost Muhammad Khan .

Passive filter is a high performance-price ratio harmonic control equipment for TPSS. Among them, C-type filter with the low fundamental power loss and high pass filtering effect is widely applied. In [3], the C-type filter is used to improve the load capacity of transformer in the non-sinusoidal condition. The C-type filter is earliest used to the harmonic control of TPSS in [4]. There is an application for single-tuned filter and C-type filter to suppress the harmonic of TPSS in [5]. A thyristor-controlled C-type filter for TPSS is proposed, which has better reactive power compensation effect, in [6]. Except TPSS, the C-type filter is also used to the harmonic control of arc furnace [7], high voltage direct current transmission system [8] and adjustable speed system [9]. What's more, the anti-resonance C-type filter is proposed in [10], [11].

So, C-type filter is used widely in harmonic control. But all articles above consider that the C-type filter has tuning-frequency [3]–[11]. The filter has a better filtering effect on harmonic corresponding to the tuning-frequency. However, we find out that the tuning-frequency may not exist.

Meanwhile, most of articles use an approximate tuning-frequency formula, which will cause the actual tuning-frequency to deviate from the expectation. Therefore, the first contribution of this work is to obtain the accurate tuning-frequency formula of the C-type filter.

In addition, the passive filter has a poor dynamic filtering effect. However, due to the multiple type of trains and working conditions, the harmonics of TPSS vary greatly. Therefore, based on the impedance-frequency index (IF) proposed in [12], the second contribution of this work is to propose a robust optimization design scheme, which make C-type filter more adaptable to great harmonic changes to its filtering effect more stable.

Finally, the effects before and after adopting the C-type filter designing by this article are compared for the four typical harmonic spectrums of TPSS, which can verify the superiority of the method.

II. HARMONIC MODEL OF TPSS

A. ALL-PARALLEL AT POWER SUPPLY SYSTEM

The all-parallel AT (Auto-Transformer) power supply system is widely used in China, which has the advantages of strong current carrying capacity, long power supply distance and small voltage loss [13]. The structure of this system is shown in Fig.1, which is mainly composed of TSS (Traction Substation), ATP (Auto-Transformer Post), SP (Section Post) and traction network. The traction network consists of up T line (T_u), down T line (T_d), up F line (F_u), down F line (F_d), and R line (up and down R lines can be combined) [14].

The electrical parts of the TSS are mainly traction transformers, feeders, and cables connected to the traction network. For connection type of traction transformers, this article focuses on the widely used V/x type, which can increase the voltage level of the power supply arm, reduce the negative sequence voltage, and save the investment of AT in TSS [15]. The AT is used to connect the same line (like T_u and F_u). The modeling method are illustrated in [16].

B. CHAIN MODEL OF TRACTION NETWORK

Traction network is a long-distance distributed parameter circuit, which is usually divided into N segments, containing N + 1 cross-sections in total. There are five nodes in each cross-section, corresponding to five lines [17]. There is a segment between the two cross-sections, which can be regarded

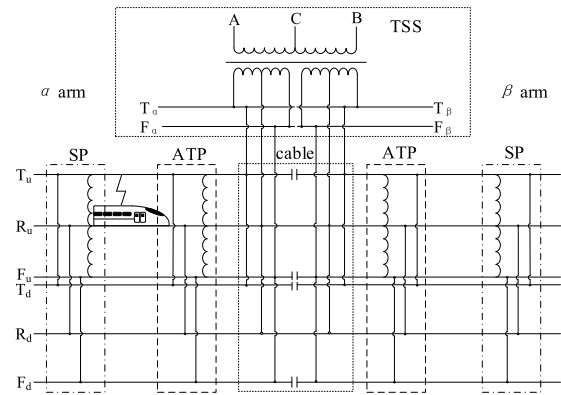


FIGURE 1. Structure of all-parallel AT power supply system.

as a lumped parameter circuit. Through the phase-to-mode transformation, the Π -type equivalent circuit of one segment traction network is derived in [18]. And its node admittance matrix is shown as

$$Y_{\pi} = \begin{bmatrix} Z_L^{-1} + \frac{Y_L}{2} & -Z_L^{-1} \\ -Z_L^{-1} & Z_L^{-1} + \frac{Y_L}{2} \end{bmatrix} \quad (1)$$

where: Z_L and Y_L are the equivalent reactance and the equivalent admittance matrix of one segment traction network. And both are square matrices. The chain Π type equivalent circuit of the entire traction network is shown in Fig.2.

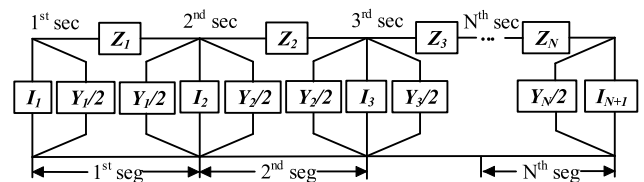


FIGURE 2. Chain Π -type mesh structure of fully parallel AT power supply system.

It can be seen from the Fig.2 that there is a common cross-section between two adjacent segments. Consequently, the nodal admittance matrix of entire system is composed of the nodal admittance matrices of each segment, which are sequentially added along the diagonal, as (2), shown at the bottom of the page.

$$\begin{bmatrix} Z_1 + \frac{Y_1}{2} & -Z_1 & 0 & \dots & 0 \\ -Z_1 & Z_1 + \frac{Y_1}{2} + \frac{Y_2}{2} + Z_2 & -Z_2 & \dots & 0 \\ 0 & -Z_2 & Z_2 + \frac{Y_2}{2} + \frac{Y_3}{2} + Z_3 & \dots & 0 \\ \dots & \dots & \dots & \dots & \dots \\ 0 & 0 & 0 & \dots & Z_N + \frac{Z_{N-1}}{2} \end{bmatrix} \quad (2)$$

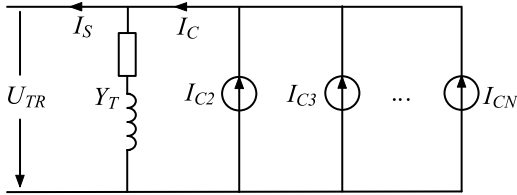


FIGURE 3. Norton harmonic model of train.

C. NORTON MODEL OF TRAIN BASED ON MEASURED DATA

The Norton harmonic model of train is illustrated as Fig.3. And it can be expressed as follow:

$$I_C = I_S + Y_T U_{TR} \tag{3}$$

where: I_S is the measured harmonic current phasor. I_C is the equivalent harmonic current source. Y_T is the equivalent admittance of train. U_{TR} is the measured harmonic voltage phasor.

In this paper, the least square method is adopted to fit the measured harmonic data of CRH2A to obtain its harmonic Norton model.

III. HARMONIC CHARACTERISTIC AND CONTROL SCHEME OF TPSS

A. HARMONIC DYNAMIC CHARACTERISTIC OF TRAIN

The harmonic source of high-speed railway TPSS includes the trains and the background harmonic from 220kV/110kV power system [19].

The PWM controlled AC-DC-AC drive mode is usually adopted in the train, which will produce characteristic harmonics near the switching frequency and its multiples. The characteristic harmonics generated by CRH2A, whose switching frequency is 1250Hz, is analyzed in [20]. When the fundamental current changes in the range of 10~230A, the HVR (Harmonic Voltage Ratio) of the 51st harmonic changes in the range of 26%~2%. So it can be seen that the characteristic harmonics will change with changes in type and operating condition of trains. For example, there are CR400BF, CRH380A, CRH380B, CRH3A, CRH3A, and CRH2A running in the Chengdu-Chongqing high-speed railway. In addition, the characteristic harmonics will Random fluctuate more severely, taking the condition of railway, the marshalling and other influencing factors into account.

B. RESONANCE DYNAMIC CHARACTERISTICS OF TPSS

In the harmonic propagation process, when the impedance of certain harmonics of the inductance and capacitance is equal, the harmonic resonance will occur, which will induce the harmonic amplification. Since the position of train is dynamic, resonance characteristics of TPSS will also change.

The model of TPSS is shown in Fig.1. Taking the SP of α arm as the coordinate zero point. The coordinates of the five stations are 0, 13, 30, 47, and 58 km. The lengths of the cables connecting the feeder (T_α , T_β , F_α and F_β) and the

TABLE 1. Parameter table of TPSS.

	Parameter	Value
Power system	Short-circuit capacity	2 GVA
	Rated voltage	220 kV
Traction transformer	Rated power	40×2 MVA
	Rated voltage	220/27.5 kV
	Short-circuit voltage	11.95%
	Short-circuit losses	113.2 kW
	Rated voltage	27.5 kV
AT in ATS and SP	Rated power	32 MVA
	Short-circuit voltage	1.6%
	Short-circuit losses	57.3 kW
Ground wire	Ground resistance	100 Ω
	Switching Frequency	1250 Hz
CRH2A Train	Resistance	3.8 Ω
	Rated voltage	25kV
	Rated power	4.8MVA
	Power factor	0.99

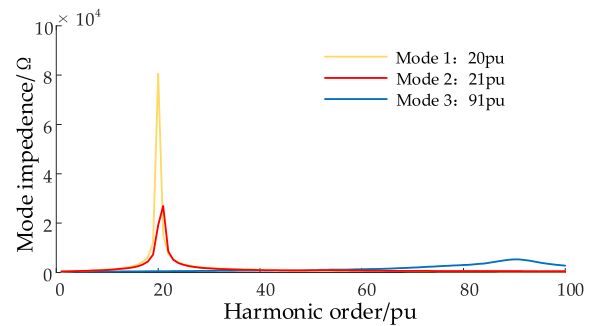


FIGURE 4. Modal analysis result graph.

traction network are 0.2, 0.5, 0.6 and 0.7 km. And there is a CRH2A train in α arm. The other parameters of TPSS are shown in Table 1.

The modal analysis result graph of TPSS (the position of train is 21 km) is shown in Fig.4 (per unit is 50Hz). The three most critical modes are shown in the figure. And each mode represents a potential resonance state of the system. Each mode has two parameters, modal frequency f_m and modal impedance Z_m . f_m represents the resonant frequency, and Z_m is equivalent to the harmonic amplification factor. The main resonance frequency is the f_m corresponding to the biggest Z_m . And this curve is also a harmonic amplification curve.

The modal analysis results of train at different position are shown in Table 2. It can be seen from the table that:

- 1) When the train at different power supply arms, the main resonance frequency varies slightly due to different parameters such as cables and lines.
- 2) The train in different position has little influence on f_m , and has great influence on Z_m .

Since the odd-order harmonic content is much larger than the even-order harmonics, although the Z_m of the

TABLE 2. Model analysis results table of train at different position.

Position of train	10 km		21 km		38 km		54 km	
	f_m	$Z_m/k\Omega$	f_m	$Z_m/k\Omega$	f_m	$Z_m/k\Omega$	f_m	$Z_m/k\Omega$
Mode 1	20	60.8	20	80.6	21	105.2	21	113.5
Mode 2	21	25.9	21	26.6	20	35.3	20	35.6
Mode 3	91	2.4	91	2.3	90	3.7	90	3.7

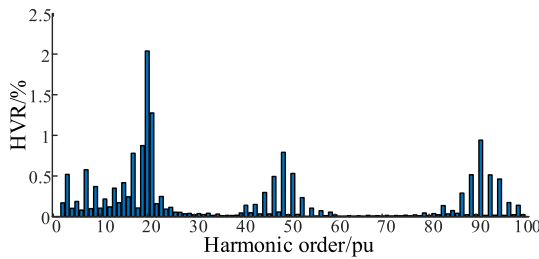


FIGURE 5. The typical harmonic spectrum of TPSS and power system connecting node (A phase).

20th harmonic may be larger than the 21st harmonic, the harmonic resonance of the 21st harmonic is still more serious. It can be seen from the Fig.5. And the 91st harmonic is the same. In addition, due to the characteristic harmonic (near the 51st harmonics) of CRH2A train, the harmonic contents near 51st are also relatively high.

C. SUMMARY OF HARMONIC DYNAMIC CHARACTERISTICS

To sum up, considering the working conditions and position of train, the harmonic dynamic characteristics of the traction power supply system are (taking the above system as an example):

- 1) The main resonance frequencies are 21st and 91st, and are basically not affected by the position of the train.
- 2) Z_m corresponding to the main resonance frequency is greatly affected by the train position. So when the train is running, the harmonic content changes significantly.
- 3) The characteristic harmonics are greatly affected by the train working conditions.

D. COMMON HARMONIC CONTROL SCHEMES OF TPSS

The harmonic suppression schemes include APF (active power filter), PPF (passive power filter) and adjusting system parameters to change resonant frequency [17].

Due to the harmonic dynamic characteristics of TPSS, APF with dynamic filter effect is the best scheme. But compared with PPF, APF has higher equipment and maintenance costs. In addition, the harmonic problem of TPSS in China is not serious. So PPF is widely used in the harmonic control scheme of TPSS in China.

According to the connection way, PPF can be divided into two types: series and parallel. The series PPF include L, LC, LCL, LLCL and so on [21], which are shown in the Fig.6. This type PPF with good high-frequency filtering effect is

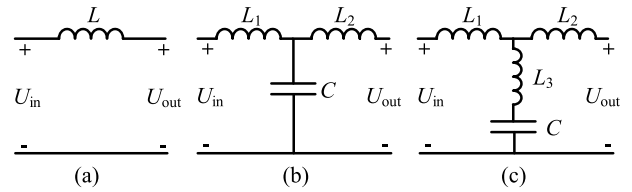


FIGURE 6. The structure of series PPF (a) L, (b) LCL (c) LLCL filter.

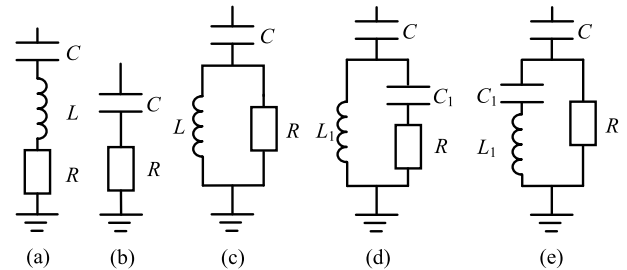


FIGURE 7. The structure of parallel PPF (a) single tuned, (b) first-order, (c) second-order, (d) third-order, and (e) C-type filter.

often used to suppress high-frequency harmonics generated by grid-connected inverters. However, in the inverter control design, the inductance and capacitance of the filter will be considered, making its design is more complicated than the parallel filter [22], [23].

The structure of parallel PPF is shown in Fig.7. First of all, the parallel PPF only needs to be connected in parallel, which makes its installation easier and has less impact on the system than the series PPF. Secondly, it can be seen from the above that the TPSS have obvious resonance frequencies. And the parallel filters such as single-tuned, double-tuned and C-type filters have a tuned frequency, which has a better suppression effect on harmonic resonance. Single-tuned filters and C-type filters are also widely used in the harmonic control of TPSS. It can be known from the Fig.5 that the frequency band of TPSS is wide. Therefore, compared with single-tuned filter, the C-type filter with zero fundamental power loss and high-frequency filtering effect is more widely used.

But most of extant filter design methods determine the parameters by mitigating the harmonic with the highest HVR. Due to the harmonic dynamic characteristics of TPSS, these methods usually do not achieve the desired filtering effect. So it is necessary to study a filter design method that is more adaptable to the random dynamic harmonics.

IV. AN EXTANT DESIGN SCHEME OF C-TYPE FILTER

The filters of TPSS are usually installed on the secondary side feeders ($T_\alpha, T_\beta, F_\alpha$ and F_β) of the traction transformer, which means that four sets of the same filter are required. In addition, their reactive power output should satisfy the requirements of reactive power compensation. Thus, the capacitance C of C-type filter in Fig.4 (e) can be expressed as following:

$$C = \frac{Q}{4\omega_1 U^2} \tag{4}$$

where: Q is the reactive power compensation required by system. ω_1 is the fundamental angular frequency. U is the rated voltage of feeder.

The C_1 and L_1 can be obtained by (5) and (6) in [5].

$$C_1 = (k_z^2 - 1)C \quad (5)$$

$$L_1 = \frac{1}{\omega_1^2 C_1} \quad (6)$$

where: k_z is the order of tuning-frequency.

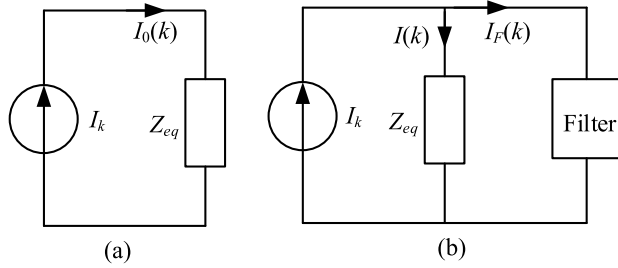


FIGURE 8. The diagram of system (a) before the connection of filter, (b) after the connection of filter.

The diagram of system after the connection of filter is illustrated in Fig.8. And $I_0(k)$ is expressed by (7).

$$I_0(k) = I(k) + I_F(k) = I(k) + I(k)Z_{eq}Y_F \quad (7)$$

where: $I_0(k)$ is the harmonic current before the connection of filter. $I(k)$ is the harmonic current after the connection of filter. $I_0(k)$ and $I(k)$ are the harmonic current measured in the secondary side of traction transformer. Y_F is the equivalent admittance of filter. Z_{eq} is the equivalent impedance of the system. k is the order of harmonic frequency, which is an integer greater than 1.

The filter index $A(k)$ is the ratio of the harmonic current after and before the connection of filter. In addition, the Z_{eq} and Y_F can be expressed as $Z_{eq} = R_{eq} + jX_{eq}$ and $Y_F = G_F + jB_F$. When the order of harmonic is high, $X_{eq} \gg R_{eq}$ and $G_F \gg B_F$. So the following equation can be obtained [4]:

$$A(k) = \frac{I(k)}{I_0(k)} = \frac{1}{1 + Z_{eq}Y_F} \approx \frac{1}{1 + jX_{eq}G_F} \quad (8)$$

It can be seen from (8) that the smaller $A(k)$, the smaller harmonic current after filter access, the stronger filter effect and $A(k)$ is inversely proportional to G_F .

The formula of equivalent conductance G_F of C-type filter is illustrated in (9).

$$G_F = \frac{R^3 X_{LC}^2 + R X_{LC}^4}{R^2 X_{LC}^4 + [R^2(X_{LC} - X_C) - X_C X_{LC}^2]^2} \quad (9)$$

where: X_{LC} is the equivalent impedance of the branch of C_1 and L_1 . $X_{LC} = (X_{L1} - X_{C1})$.

By setting the derivative of G_F in terms of R equal to zero, the extreme values R_p of G_F can be obtained like (10).

$$R_p = \pm \frac{X_C X_{L1}}{X_C - X_{L1}} \quad (10)$$

When R tends to 0 or infinity, the limit of G_F is 0. $|R_p|$ is value of R for which G_F is maximum. At this point, G_F is the largest and $A(k)$ is the smallest, which means the filtering effect of the filter is the best.

It should be noted that $A(k)$ represents the filtering effect in a specific harmonic. k_{max} is frequency order with the highest HVR. When designing the filter parameters, k is k_{max} . But in the condition that k_{max} is variable, the filtering effect will decrease.

V. IMPROVED DESIGN SCHEME OF C-TYPE FILTER

There are three problems in the design scheme of section IV:

1) Equation (5) is obtained by (11). But (11) is established when the filter resistance R is infinity, which means all the current flowing through C passes through the branch of L_1 and C_1 . Because the R can not be infinity, the (5) is an approximate formula. Therefore, the filter designed by (5) has a deviation from the expectation and even no tuning-frequency. However, almost all studies on C-type filters in the introduction are based on (11).

$$X_{L1} - X_{C1} - X_C = 0 \quad (11)$$

2) The optimal selection of parameters is based on the $A(k)$. When the harmonic spectrum of the system changes severely, especially when the harmonic frequency with the highest HVR changes, the filtering effect will be significantly reduced.

3) $A(k)$ reflects the filtering effect of the filter installation position. But the filter of TPSS is generally installed on the secondary side of the traction transformer. However, it is paid more attention to the harmonics of the coupling point between the power system and TPSS. The harmonic suppression scheme based on $A(k)$ may not be an optimal scheme for the coupling point.

Therefore, this article will accurately derive the tuning-frequency expression of the C-type filter. What's more, the IF is introduced, which can reflect the overall harmonics at the coupling point. Based on these, a more robust filtering scheme is proposed.

A. DERIVATION OF TUNING-FREQUENCY

In a series circuit composed of an inductor and a capacitor, when the capacitive reactance and the inductive reactance are equal at a certain harmonic order, the reactance of the circuit is 0. This situation is called series resonance. The parallel resonance is the same, but the reactance of the circuit is ∞ . The resonance frequency of filter circuit is also called as tuning-frequency. The tuning-frequency of C-type filter is discussed below by the mathematical model.

Setting the impedance of filter $Z_F = R_F + jX_F$, they can be expressed as following:

$$X_F = \frac{R^2 X_{LCk}}{R^2 + X_{LCk}^2} - X_C, \quad R_F = \frac{R X_{LCk}^2}{R^2 + X_{LCk}^2} \quad (12)$$

For the zero fundamental power loss, (6) still holds. Setting $C_1 = \alpha C$ and substituting it into (6), (13) can be obtained.

$$L_1 = \frac{1}{\omega_1^2 \alpha C} \quad (13)$$

X_{LCk} is X_{LC} in the k -order harmonic, which is expressed as:

$$X_{LCk} = \frac{(k - k^{-1})}{\alpha} X_C \quad (14)$$

where: X_C is the fundamental reactance of capacitor C (Absolute value). i.e., $X_C = 1/(\omega_1 C)$.

By substituting the (14) into (12), we obtain:

$$X_F = \frac{(\alpha R^2 X_C - X_C^3)k^4 - [\alpha(\alpha + 1)R^2 X_C - 2X_C^3]k^2 - X_C^3}{X_C^2 k^5 + (\alpha^2 R^2 - 2X_C^2)k^3 + X_C^2 k} \quad (15)$$

For the denominator of X_F (discussing the poles of X_F), when the pole k_p is in the interval $(1, \infty)$, X_F will have a maximum, and k_p corresponds to the order of parallel tuning-frequency. Near k_p , the filter has almost no filtering effect. Therefore, it should be avoided during parameter design. Setting the largest pole less than 1, that is shown as (16).

$$k_p = \sqrt{\frac{-(\alpha^2 R^2 - 2X_C^2) + \alpha R \sqrt{\alpha^2 R^2 - 4X_C^2}}{2X_C^2}} < 1 \quad (16)$$

Solving (16), the condition of the largest pole less than 1 is that $X_C > 0$. So there must be no parallel tuning-frequency for C-type filter.

For the numerator of X_F (discussing the zeros of X_F), when the zero k_z is in the interval $(1, \infty)$, X_F will have a zero value, and k_z corresponds to the order of series tuning-frequency. Near k_z , the filter has best filtering effect. So the parameter design should ensure the existence of the series tuning-frequency.

In the case that the quartic coefficient is greater than 0, the following can be obtained easily.

$$\alpha > \frac{X_C^2}{R^2} \Leftrightarrow R > \frac{1}{\sqrt{\alpha}} X_C \quad (17)$$

According to the Vieta theorem, the relation of two roots is expressed as following:

$$k_1^2 k_2^2 = -\frac{X_C^2}{\alpha R^2 - X_C^2} < 0 \quad (18)$$

It can be known from (18) that there are a set of conjugate zeros and a set of opposite zeros. Therefore, there must be a zero in the interval $(0, \infty)$, when $\alpha > (X_C/R)^2$. The curve of X_F numerator in this case is shown in Fig.9(a).

But k is in the interval $(1, \infty)$, the above conclusion is not sufficient. Therefore, it is required to discuss the existence of zero in the interval $(1, \infty)$.

The zeros k_z can be expressed as following:

$$k_z = \sqrt{\frac{\alpha(\alpha + 1)R^2 - 2X_C^2 \pm \alpha R \sqrt{\alpha^2(\alpha + 1)^2 R^2 - 4X_C^2}}{2(\alpha R^2 - X_C^2)}} \quad (19)$$

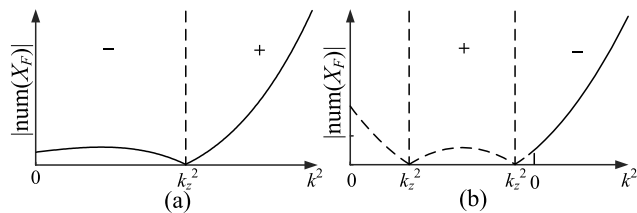


FIGURE 9. The curve of X_F numerator changing with k when (a) $\alpha > (X_C/R)^2$ and (b) $\alpha < (X_C/R)^2$.

Setting $k_z > 1$, (20) can be obtained.

$$R > \frac{1}{\sqrt{\alpha}} X_C \quad (20)$$

It can be reflected from (17) and (20) that in this case, there must be a series tuning-frequency for C-type filter. Transforming (19), the expression of α can be obtained as following:

$$\alpha = \frac{(k_z^2 - 1)(k_z R + \sqrt{k_z^2 R^2 - 4X_C^2})}{2k_z R} \quad (21)$$

It should be noticed that:

$$k_z^2 R^2 - 4X_C^2 > 0 \quad (22)$$

In the case that the quartic coefficient is less than 0, the following can be obtained easily:

$$\alpha < \frac{X_C^2}{R^2} \Leftrightarrow R < \frac{1}{\sqrt{\alpha}} X_C \quad (23)$$

But when $k = 0$, the value of the numerator is $-X_C^3 < 0$. So the zeros must be on the negative semi-axis of k , like Fig.9(b). Therefore, in this case, there must be no tuning-frequency in the interval $(1, \infty)$. The curve of X_F changing with k is shown as Fig.10.

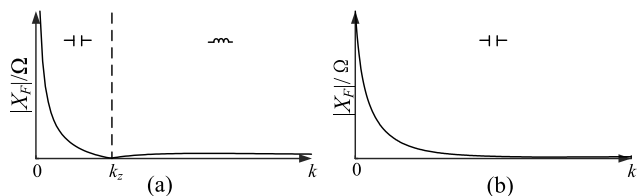


FIGURE 10. The curve of X_F changing with k when (a) $\alpha > (X_C/R)^2$ and (b) $\alpha < (X_C/R)^2$.

The expression of equivalent resistance R_F is shown as following:

$$R_F = \frac{RX_C^2(k^2 - 1)^2}{X_C^2 k^4 + (\alpha^2 R^2 - 2X_C^2)k^2 + X_C^2} \quad (24)$$

The discussion of R_F denominator is the same as X_F . It can be seen that in fundamental frequency $R_F = 0$ which means the fundamental power loss is zero. What's more, X_F in the high frequency is almost zero. So the equivalent resistance R_F at high frequency has a greater impact on the filtering effect.

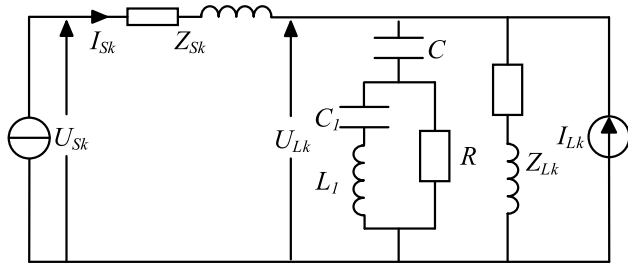


FIGURE 11. System diagram after C-type the connection of filter.

B. IMPEDANCE-FREQUENCY INDEX

The system diagram after the connection of C-type filter is illustrated in Fig.11. According to the installation position of the filter, it can be known that Z_{Sk} includes the impedance of the traction transformer and power system. And Z_{Lk} includes the impedance of the traction net and train. In the k -order harmonic, there are equations as following [12]:

$$\begin{cases} I_{Sk} = \frac{U_{Sk}(Z_{Fk} + Z_{Lk}) + I_{Lk}(Z_{Fk}Z_{Lk})}{Z_{Sk}Z_{Fk} + Z_{Sk}Z_{Lk} + Z_{Fk}Z_{Lk}} \\ U_{Lk} = U_{Sk} - I_{Sk}Z_{Sk} \end{cases} \quad (25)$$

Transforming (25), the (26) can be obtained.

$$\frac{I_{Sk}}{I_{Lk}} = \frac{Z_k}{Z_{Sk}} \quad (26)$$

where: I_{Sk} is the k -order harmonic current of power system. I_{Lk} is the k -order load harmonic current in the secondary side of traction transformer. Z_k is the k -order harmonic impedance of whole system. It can be expressed as following:

$$Z_k = \frac{Z_{Sk}Z_{Fk}Z_{Lk}}{Z_{Sk}Z_{Fk} + Z_{Sk}Z_{Lk} + Z_{Fk}Z_{Lk}} \quad (27)$$

It can be seen from (27) that when I_{Lk} is constant, the smaller Z_k , the smaller I_{Sk} flowing to the power system side, and the stronger filtering ability of the filter. Therefore, IF is introduced as (28):

$$IF = \sum_{k=1}^n |Z_k| \quad (28)$$

where: n is the maximum harmonic order cared.

Because IF considers all cared harmonic orders, the overall filtering effect designed with IF will be better than the previous scheme. What's more, it is relatively less affected by changes in the harmonic spectrum.

VI. HARMONIC CONTROL SCHEME FOR TPSS

A. PARAMETER DESIGN OF THE TWO SCHEMES

According Table 1, the rated traction power of CRH2A train is 4.8MVA, and the power factor is 0.99. According to (4), it can be calculated that $C = 0.72\mu\text{F}$. According to Section III, the system has high harmonic resonant at the 21th harmonic. Thus, the tuning-frequency order is selected as 21th. According to (22), it can be obtained that $R > 442.1\Omega$.

It can be known form (24) that R_F will approach R in the high frequency. So the bigger R , the worse high frequency

filtering effect. Therefore, the result of the optimization algorithm must be close to the lower limit, and a higher upper limit will increase the calculation amount of the optimization algorithm. According to a large number of optimization calculations, it is most appropriate to select the upper limit as 1.1~1.2 times than lower limit. So The value range of R is (442.1, 500].

Combining (13) and (21), the expression of Z_F changing with R can be obtained. Then substituting Z_F into (27) and (28), the expression of IF changing with R can be get. Since it is a nonlinear equation with constraints, this paper uses an Firefly Algorithm (FFA) to find the optimal solution of the R [24]. This algorithm is based on following concepts: each firefly is attractive, whose attraction is proportional to its brightness and inverse proportional to the distance. In addition, the fireflies will move towards another firefly which is most attractive to it. The algorithm is as following:

Each firefly is a solution. The attraction A_{ij} of firefly i to firefly j is expressed as:

$$A_{ij} = B_i e^{-\gamma r_{ij}^2} \quad (29)$$

where: B_i is the brightness of firefly i , which is proportional to the objective function. γ is the absorption coefficient, which indicates how the attraction between fireflies weakens with distance. r_{ij} is the distance between two fireflies, which is expressed as:

$$r_{ij} = \sqrt{\sum_{k=1}^M (x_i(k) - x_j(k))^2} \quad (30)$$

where: x_i is the position of the firefly i , which is also the variable of objective function. M is the dimension of variable.

Assuming the firefly j is the most attractive to firefly i , the new position after it moving is expressed as:

$$x_i^{t+1} = x_i^t + A_{ij}^t (x_j^t - x_i^t) \text{rand}(0, 1) + m \text{Drand}(-1, 1) \quad (31)$$

where: $\text{rand}(a, b)$ is a random value within the range (a, b). m is the mutation coefficient. D is the difference between maximum and minimum. The superscript t is the number of iteration.

The number of fireflies is 50. The number of iteration is 100. The mutation coefficient m is 0.01. The absorption coefficient γ is 0.8. When $R \in (442.1, 500]$, the FFA finds the best value of R is 451.18Ω. Substituting R , k_z , and C into (23) and (15) can obtain the C-type filter parameters.

For the original scheme, since the tuning-frequency is the 21th harmonic, the k of $A(k)$ is selected as 91th to obtain the best filtering effect on the 91st harmonic. The parameters of the two schemes are shown in Table 3.

B. FILTER EFFECT ANALYSIS

The R_F curves of the two schemes are shown in Fig.12(a). The equivalent resistance of the two schemes is 0 in the fundamental frequency, which means the fundamental power

TABLE 3. C-type filter parameter table.

	Original Scheme	Improve Scheme
k_f /pu		21
C / μ F		0.72
C_1 / μ F	287.3	172.4
L_1 /mH	35.3	58.8
R / Ω	245.5	451.2

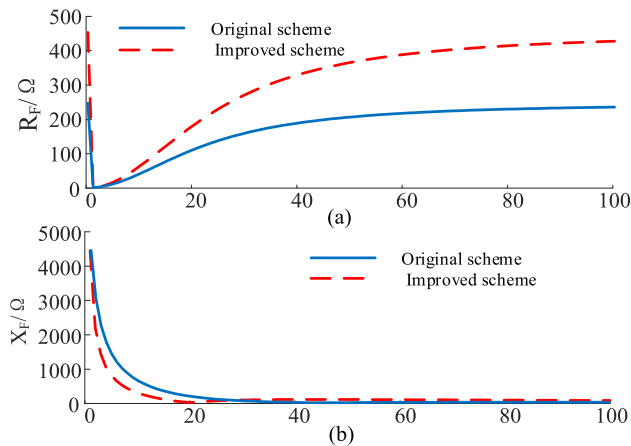


FIGURE 12. The (a) R_F and (b) X_F curves of the two schemes.

loss can be ignored. The X_F curves of the two schemes are shown in Fig.12(b). It can be seen that there is no tuning-frequency for the original scheme. So, the suppression effect near the expected tuning-frequency will be worse.

According to the two curves it can be seen that $R_F \ll X_F$ in the low frequency. Therefore, X_F determines the low frequency suppression effect, while the high frequency is the opposite. So, the high frequency suppression effect of the original scheme is better than that of the improved scheme. However, because of larger R , formula (19) is established, which reflects there is a zero for X_F at low frequencies. Thence, the low frequency equivalent reactance of the improved scheme is much smaller than the original scheme, and its low frequency filtering effect is better than that of the original scheme.

C. CASE ANALYSIS

Base on the model of TPSS in Section III, the above two filter schemes are analyzed. In the following, the harmonic spectrum is divided into three areas: low frequency area (below the 25th harmonic), characteristic harmonic area (near the 50th harmonic) and high-frequency area (above the 75th harmonic).

Based on Section III, when the train harmonics and system harmonic amplification are different in the low and high frequencies, the harmonic spectrums may be very different. For example, when the train position causes the large amplification of 21st and 91st harmonic but the train working condition

causes small characteristic harmonics, the harmonic spectrum will be shown like *Case 1*.

Case 1: Before the connection of filter, the *HVR* of characteristic harmonic is low, and the *HVR* of low-order harmonic is higher than the high-order harmonic.

The harmonic spectrum of case 1 is shown in Fig.13. The THD_u (total harmonic voltage distortion) of the improved scheme is lower than the original scheme. Therefore, the filtering effect of the improved scheme is better.

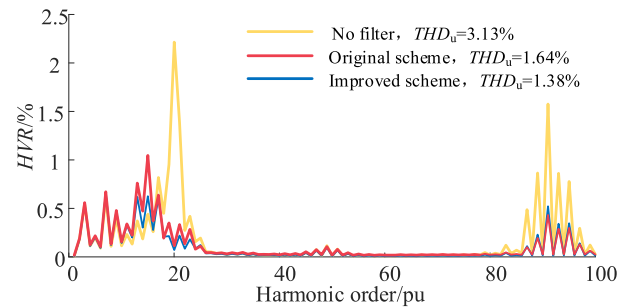


FIGURE 13. A-phase bus harmonic spectrum diagram (case 1).

Case 2: Before the connection of filter, the *HVR* of characteristic harmonic is low, and the *HVR* of high-order harmonic is higher than the low-order harmonic.

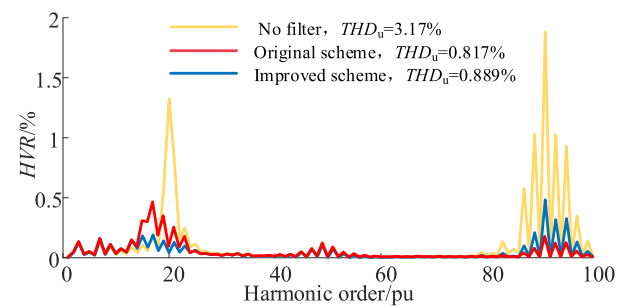


FIGURE 14. A-phase bus harmonic spectrum diagram (case 2).

The harmonic spectrum of case 2 is shown in Fig.14. In this case, since the *HVR* of 91th and nearby harmonics is significantly higher than other frequency bands, and the original scheme selects the minimum value of $A(k)$ in the 91th harmonic. In this case, the filtering effects of original scheme in the high frequency area and the overall are better than the improved scheme. Therefore, When the *HVR* of the selected area of $A(k)$ is higher, the filtering effect of the original scheme is better.

Case 3: Before the connection of filter, the *HVR* of characteristic harmonic is higher, and the *HVR* of low-order harmonic is higher than the high-order harmonic.

The harmonic spectrum of case 3 is shown in Fig.15. This case is similar to case 1, and the filtering effect of the improved scheme is better than that of the original scheme.

Case 4: Before the connection of filter, the *HVR* of characteristic harmonic is higher, and the *HVR* of high-order harmonic is higher than the low-order harmonic.

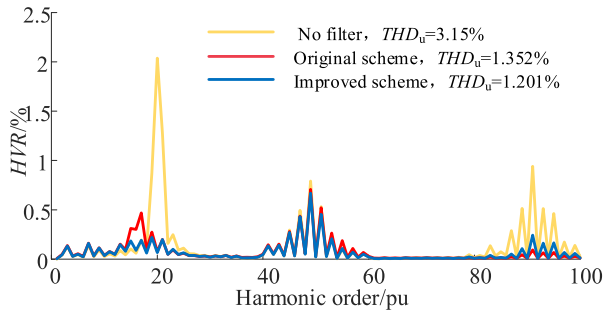


FIGURE 15. A-phase bus harmonic spectrum diagram (case 3).

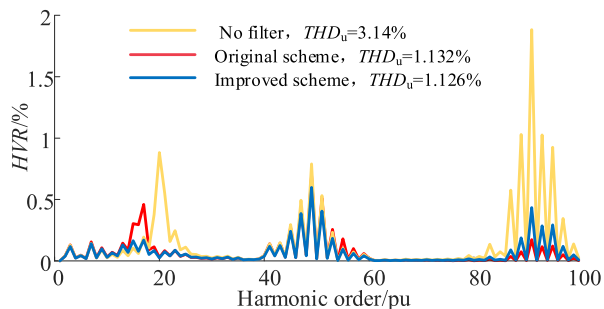


FIGURE 16. A-phase bus harmonic spectrum diagram (case 4).

The harmonic spectrum of case 4 is shown in Fig. 16. In this case, since the improvement scheme has better characteristic harmonic control effect than the original scheme, compared with Case 2, the overall control effect of the two schemes is basically the same

The filtering efficiency η [5] can be expressed as:

$$\eta = \left(1 - \frac{THD_a}{THD_b}\right) \times 100\% \quad (32)$$

where: THD_a is the THD_u after the connection of filter. THD_b is the THD_u before the connection of filter.

η can reflect the filtering effect. The more η , the better filtering effect. The THD before or after the connection of filter and for each case is illustrated in Table 4.

TABLE 4. Summary table of THD and η for each case.

	No filter	Original scheme		Improved scheme	
	$THD/\%$	$THD/\%$	η	$THD/\%$	η
Case 1	3.13	1.64	47.60%	1.281	59.07%
Case 2	3.17	0.817	74.23%	0.889	71.96%
Case 3	3.15	1.392	55.81%	1.201	61.87%
Case 4	3.14	1.132	63.95%	1.126	64.14%

Except for case 2, the filtering efficiency of the improved scheme is generally better than that of the original scheme, and the filtering efficiency of the improved scheme (62%~72%) is more stable than the original scheme (47%~75%), which means that it is relatively less affected by spectrum changes. Because the improved scheme guarantees

the existence of the tuning-frequency, the filtering effect near the tuning-frequency is better than the original scheme.

VII. CONCLUSION

Based on mathematical derivation, this paper obtains the precise parameter design formula of C-type filter, and proposes a robust optimization design scheme of C-type filter in TPSS that takes into account the random dynamic characteristics of harmonics. These conclusions are as follows:

1) When R is small, the tuning-frequency will deviate from the expected value and even there will be no tuning-frequency. Therefore, using an approximate tuning-frequency calculation formula may result in the loss of the tuning-frequency, and reduce the filtering effect near the tuning-frequency.

2) The improved parameter design scheme ensures the existence of the tuning-frequency, which will make R larger. So the high-frequency suppression effect is slightly lower than the original scheme. But due to the existence of the low-frequency tuning point, the low-frequency equivalent reactance is smaller than the original design, which causes the better low frequency suppression effect.

3) Comparing the results of the four cases, it can be seen that the filtering efficiency of the scheme in this paper is higher than that of the existing methods, and the filtering efficiency fluctuates less with the change of the frequency spectrum. So its adaptability is stronger.

REFERENCES

- [1] J. Zhu, H. Hu, Z. He, X. Guo, and W. Pan, "A power-quality monitoring and assessment system for high-speed railways based on train-network-data center integration," *Railway Eng. Sci.*, vol. 29, no. 1, pp. 30–41, Mar. 2021, doi: 10.1007/s40534-020-00229-4.
- [2] W. C. Cui, M. G. Liu, and J. W. Zhen, "Research on the mechanism and characteristics of interharmonics in traction power supply system of high-speed railway," *Railway Standard Des.*, vol. 65, no. 6, pp. 139–146, Jun. 2021, doi: 10.13238/j.issn.1004-2954.202007140008.
- [3] M. E. Balci, "Optimal C-type filter design to maximize transformer's loading capability under non-sinusoidal conditions," *Electr. Power Compon. Syst.*, vol. 42, no. 14, pp. 1565–1575, Sep. 2014, doi: 10.1080/15325008.2014.943827.
- [4] H. Hu, Z. He, and S. Gao, "Passive filter design for China high-speed railway with considering harmonic resonance and characteristic harmonics," *IEEE Trans. Power Del.*, vol. 30, no. 1, pp. 505–514, Feb. 2015, doi: 10.1109/TPWRD.2014.2359010.
- [5] Y. Shao, L. H. Chen, H. T. Hu, Z. Y. He, and K. Wang, "Harmonic suppression of high speed railway traction power supply system based on combination of Chebyshev filter and single tuned filter," *J. China Railw. Soc.*, vol. 40, no. 4, pp. 52–59, Apr. 2018, doi: 10.3969/j.issn.1001-8360.2018.04.008.
- [6] M. W. Chen, Y. Y. Chen, and M. C. Wei, "Modeling and control of a novel hybrid power quality compensation system for 25-kV electrified railway," *Energies*, vol. 40, no. 4, p. 23, Aug. 2019, doi: 10.3390/en12173303.
- [7] A. G. Lange and G. Redlarski, "Selection of C-type filters for reactive power compensation and filtration of higher harmonics injected into the transmission system by arc furnaces," *Energies*, vol. 13, no. 9, p. 19, May 2020, doi: 10.3390/en13092330.
- [8] R. Zhen, Y. Zeng, and B. M. Dai, "Optimization model and algorithm of type-C damped filter in high voltage direct current transmission system," *Proc. CSEE*, vol. 22, no. 12, pp. 124–127, Dec. 2002, doi: 10.13334/j.0258-8013.pcsee.2002.12.025.
- [9] C. S. A. Mboving and Z. Hanzelka, "Application of C-type filter to DC adjustable speed drive," in *Proc. Modern Electr. Power Syst. (MEPS)*, Jul. 2015, pp. 1–7, doi: 10.1109/MEPS.2015.7477172.

- [10] A. Lamlo, A. Ibrahim, M. E. Balci, A. Karadeniz, and S. H. E. A. Aleem, "Optimal design and analysis of anti-resonance C-type high-pass filters," in *Proc. IEEE Int. Conf. Environ. Electr. Eng. IEEE Ind. Commercial Power Syst. Eur. (EEEIC/ICPS Europe)*, Jun. 2017, pp. 1–6, doi: [10.1109/EEEIC.2017.7977602](https://doi.org/10.1109/EEEIC.2017.7977602).
- [11] G. Zhang, Y. Wang, W. Xu, and E. Sittler, "Characteristic parameter-based detuned C-Type filter design," *IEEE Power Energy Technol. Syst. J.*, vol. 5, no. 2, pp. 65–72, Jun. 2018, doi: [10.1109/JPEETS.2018.2825279](https://doi.org/10.1109/JPEETS.2018.2825279).
- [12] S. H. E. A. Aleem and A. F. Zobaa, "Optimal C-type filter for harmonics mitigation and resonance damping in industrial distribution systems," *Electr. Eng.*, vol. 99, no. 1, pp. 107–118, Mar. 2017, doi: [10.1007/s00202-016-0406-1](https://doi.org/10.1007/s00202-016-0406-1).
- [13] B. Wang, H. T. Hu, S. B. Gao, X. D. Han, and Z. Y. He, "Power flow calculation and analysis for high-speed railway traction network under regenerative braking," *China Railw. Sci.*, vol. 35, no. 1, pp. 86–93, Jan. 2014, doi: [10.13334/j.0258-8013.pcsee.2012.13.011](https://doi.org/10.13334/j.0258-8013.pcsee.2012.13.011).
- [14] H. Lee, C. Lee, G. Jang, and S.-H. Kwon, "Harmonic analysis of the Korean high-speed railway using the eight-port representation model," *IEEE Trans. Power Del.*, vol. 21, no. 2, pp. 979–986, Apr. 2006, doi: [10.1109/MEPS.2015.7477172](https://doi.org/10.1109/MEPS.2015.7477172).
- [15] S. C. Xiao, "Application of unequal capacity V/X connection traction transformer on secondary side," *Electr. Eng.*, no. 20, pp. 120–121, Oct. 2020, doi: [10.19768/j.cnki.dgjs.2020.20.050](https://doi.org/10.19768/j.cnki.dgjs.2020.20.050).
- [16] M. L. Wu, "Research on electrical parameters and mathematical model of traction power supply system," Ph.D. dissertation, Dept. Elect. Eng., Beijing Jiaotong Univ., Beijing, China, 2006.
- [17] H. T. Hu, "Harmonic propagation and resonance analysis for traction power supply system of high-speed railway," Ph.D. dissertation, Dept. Elect. Eng., Southwest Jiaotong Univ., Chengdu, China, 2014.
- [18] M. Wu, "Uniform chain circuit model for traction networks of electric railways," *Proc. CSEE*, vol. 30, no. 28, pp. 52–58, Oct. 2010, doi: [10.13334/j.0258-8013.pcsee.2010.28.004](https://doi.org/10.13334/j.0258-8013.pcsee.2010.28.004).
- [19] H. Hu, Y. Shao, L. Tang, J. Ma, Z. He, and S. Gao, "Overview of harmonic and resonance in railway electrification systems," *IEEE Trans. Ind. Appl.*, vol. 54, no. 5, pp. 5227–5245, Sep. 2018, doi: [10.1109/TIA.2018.2813967](https://doi.org/10.1109/TIA.2018.2813967).
- [20] S. Yang and M. Wu, "Study on harmonic distribution characteristics and probability model of high speed EMU based on measured data," *J. China Rail Soc.*, vol. 32, no. 3, pp. 33–38, Jun. 2010, doi: [10.3969/j.issn.1001-8360.2010.03.006](https://doi.org/10.3969/j.issn.1001-8360.2010.03.006).
- [21] D. Z. Xu, F. Wang, and Y. Ruan, "Passive damping of LCL, LLCL and LLCL filters," *Proc. CSEE*, vol. 35, no. 18, pp. 4725–4735, Sep. 2015, doi: [10.13334/j.0258-8013.pcsee.2015.18.020](https://doi.org/10.13334/j.0258-8013.pcsee.2015.18.020).
- [22] C. L. Bao, X. B. Ruan, X. H. Wang, D. H. Pan, W. W. Li, and K. L. Weng, "Design of grid-connected inverters with LCL filter based on PI regulator and capacitor current feedback active damping," *Proc. CSEE*, vol. 32, no. 25, pp. 133–142, Sep. 2012, doi: [10.13334/j.0258-8013.pcsee.2012.25.022](https://doi.org/10.13334/j.0258-8013.pcsee.2012.25.022).
- [23] F. Liu, X. M. Zha, and S. X. Duan, "Design and research on parameter of LCL filter in three-phase grid-connected inverter," *Trans. China Electrotech. Soc.*, vol. 25, no. 3, pp. 10–116, Mar. 2010, doi: [10.19595/j.cnki.1000-6753.tces.2010.03.017](https://doi.org/10.19595/j.cnki.1000-6753.tces.2010.03.017).
- [24] R. Klempka, Z. Waradzyn, and A. Skala, "Application of the firefly algorithm for optimizing a single-switch class e ZVS voltage-source inverter's operating point," *Adv. Electr. Comput. Eng.*, vol. 18, no. 2, pp. 93–100, 2018, doi: [10.4316/AECE.2018.02012](https://doi.org/10.4316/AECE.2018.02012).



HEXIANG WU received the B.S. degree in traffic signal and control from Shanghai Tiedao University, Shanghai, China. He is currently working at China Railway Signal & Communication (Changsha) Railway Traffic Control Technology Company Ltd., as a Senior Engineer. His research interest includes intelligent railway power supply systems.



LIYONG ZENG received the B.S. degree in electrical engineering and automation from Wuhan University, Wuhan, Hubei, China. He is currently working at China Railway Signal & Communication (Changsha) Railway Traffic Control Technology Company Ltd., as a Senior Engineer. His research interest includes intelligent railway power supply systems.



QINGSHUO REN received the B.S. degree in electrical engineering from Dalian Jiaotong University, Dalian, Liaoning, China, in 2019. He is currently pursuing the M.S. degree in electrical engineering with Southwest Jiaotong University, Chengdu, Sichuan, China. His research interests include power quality and operation quality evaluation of traction power supply systems.



LEI AI received the B.S. degree in electrical engineering from Southwest Jiaotong University, Chengdu, Sichuan, China, in 2020, where he is currently pursuing the M.S. degree in electrical engineering. His research interests include harmonic analysis and control of traction power supply systems.

• • •